

The Effect of Highly Ionising Events on the APV25 Readout Chip

R. Bainbridge*

On behalf of the CMS Tracker Collaboration

* Blackett Laboratory, Imperial College, London, UK
r.bainbridge@ic.ac.uk

Abstract

Inelastic nuclear interactions in silicon sensors can produce highly ionising particles and result in signals equivalent of up to ~ 1000 minimum ionising particles. These rare events have been observed to cause measurable deadtime in all 128 channels of the CMS Tracker APV25 front-end readout chip. Analysis of beam test data, laboratory measurements and simulation studies have provided measurements of both the rate at which non-negligible deadtime occurs and the most probable deadtime resulting from a highly ionising event. Laboratory measurements also predict that through a suitable choice of a front-end hybrid resistor, the deadtime may be reduced. The inefficiency due to highly ionising events is predicted to be at the sub-percent level in CMS.

I. HIGHLY IONISING EVENTS AND THE DEADTIME MECHANISM

Simulation studies [1] have shown that essentially all inelastic nuclear interactions between pions and silicon generate a highly ionising event. Energy depositions of up to ~ 100 MeV in $500 \mu\text{m}$ of silicon are predicted. Nuclear recoils result in highly localised ($< 100 \mu\text{m}$) energy depositions of up to a few tens of MeV. Light nuclear fragments may travel up to a few mm and can also be highly ionising. Events with the largest energy depositions always involve several particles.

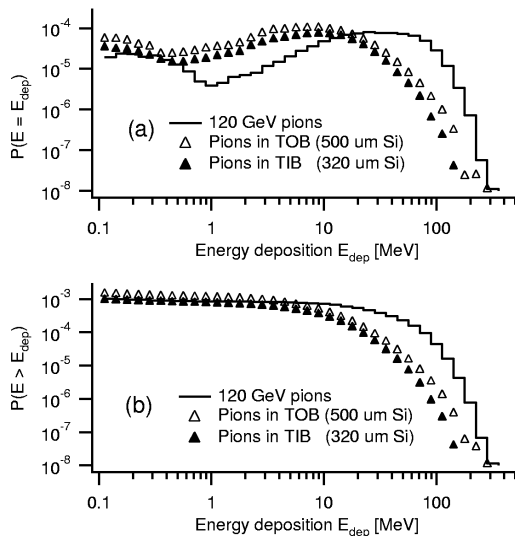


Figure 1: (a) Differential and (b) cumulative energy deposition spectra for pions with 120 GeV and energy spectra as predicted for CMS Tracker Inner and Outer Barrel regions. Taken from [1].

Figure 1 (a) shows the probability of a π -Si interaction resulting in an energy deposition E_{DEP} [MeV] for 120 GeV pions at normal incidence, and for pions with their predicted energy spectra in the Tracker Inner and Outer Barrel regions and an isotropic angular distribution. Figure 1 (b) shows the probability of a π -Si interaction resulting in an energy deposition E_{DEP} or greater, for the same pion energy and angular distributions.

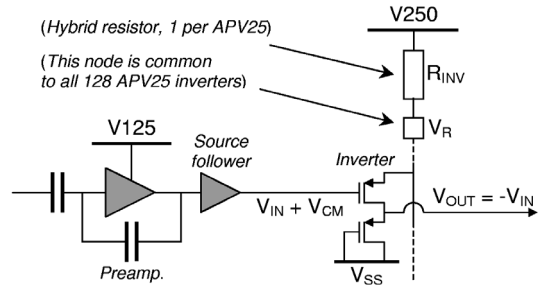


Figure 2: Front-end amplifying stages of a single APV25 channel.

The bulk of the signal resulting from a highly ionising event is usually collected on one or two channels and the signal is often sufficient to saturate the preamplifier of these channels, but the design of the biasing at the APV25 inverter stage results in all 128 channels being affected. The effect was first observed during the X5 beam test in October 2001, in which 6 silicon sensors, instrumented with the APV25, were exposed to a 120 GeV pion beam with a 25 ns bunch structure.

The APV25 inverter stage is powered by the V250 power rail via an external hybrid resistor, R_{INV} (see figure 2). This scheme provides on-chip common mode subtraction as any common mode signal, V_{CM} , is not seen on the internal inverter output nodes, but on the external resistor ($V_{\text{R}} \approx V_{\text{CM}}$). This results in a very stable baseline during normal operation. However, a large signal at one or more of the inverter input nodes, V_{IN} , will drive down V_{R} and, consequently, the inverter output of all the other channels (as V_{R} is common to all channels). A sufficiently large signal will result in non-negligible *deadtime*, during which all 128 channels are insensitive to normal signals, until the signal dissipates sufficiently for the chip to recover. The magnitude of the deadtime is dependent on the signal.

II. X5 BEAM TEST

The aim of the October 2001 beam test was to operate a near final-version synchronous readout system under LHC-like operating conditions. Six modules, each comprising of a 500 μm thick sensor instrumented with 4 APV25 chips, were

exposed to a 120 GeV pion beam with a 25 ns particle bunch structure, similar to that used during the May 2000 beam test [2]. High instantaneous intensities, necessary for high trigger-rate conditions, were achieved by delivering pions (or muons) to the target area in *trains* of ~ 60 consecutive RF buckets. Bunch trains, separated in time by the SPS orbit period of 23.1 μs , arrived repeatedly at the target area throughout a *spill* of duration ~ 2 s. Coincident signals from 2 scintillators placed upstream of the detectors identified occupied RF buckets and provided the triggers for the readout system.

A. HIP rate measurement

If a trigger is coincident in time with the occurrence of a highly ionising event, the analogue data from the affected APV25 chip exhibit large (and often truncated) signals in several channels and a negative shift in all other channels. If the energy deposition is sufficiently large then the output of all channels (not seeing the large signal) is driven to the lower limit of the APV25 dynamic range. Consequently, minimum ionising particle signals present in any of the channels (along with the pedestal structure observed across the 128 channels) are suppressed, resulting in deadtime. Figure 3 shows an example of a highly ionising event; the output of one APV25 in the third module exhibits a cluster of adjacent strips containing large signals and a shifted baseline. A high level of activity is also observed in the modules downstream.

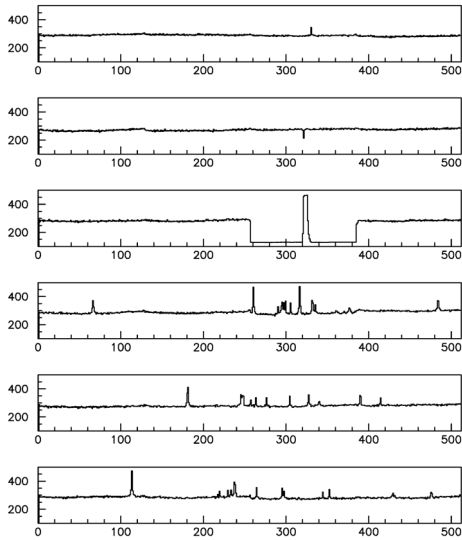


Figure 3: Raw analogue data from 6 modules, displaying a highly ionising event.

The distribution of common mode (CM) levels is shown in figure 4. Increasingly large energy depositions from highly ionising events result in increasingly shifted baselines, producing the negative CM tail. The pronounced peak found at the end of the tail is due to the limited dynamic range of the APV25, providing an upper limit on the maximum observable CM shift.

Figure 5 shows cluster size [strips] versus cluster signal [ADC counts] for clusters found in frames with $\text{CM} < -140$ ADC counts (i.e. with baselines at or near the lower limit of the available dynamic range). Two populations of clusters can be identified: those produced by minimum ionising particles,

which typically contain signals of ~ 100 ADC counts in one or two strips; and those produced by highly ionising particles, which typically contain signals of several thousand ADC counts spread across several strips. It is important to note that the magnitude and spatial distribution of the energy depositions in the silicon sensors cannot be deduced from the data, as signals are frequently truncated due to the limited dynamic range of the APV25 and inter-strip capacitive coupling ‘smears’ the signal over an increased number of strips.

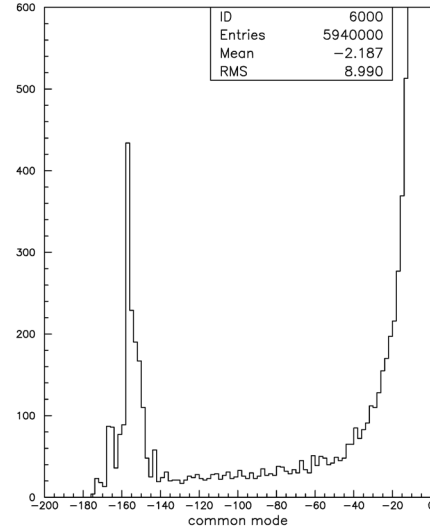


Figure 4: Common mode distribution [ADC counts].

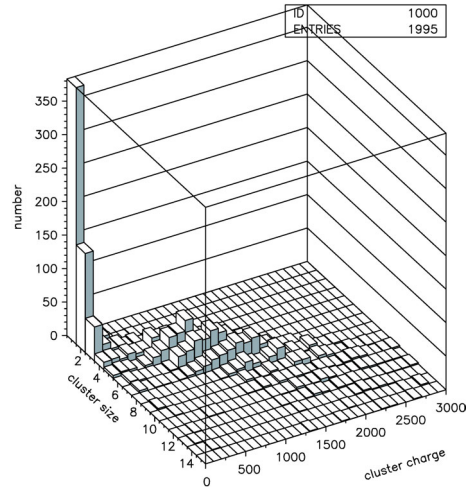


Figure 5: Cluster size [strips] versus cluster charge [ADC counts], in frames with $\text{CM} < -140$ ADC counts.

Highly ionising events causing non-negligible deadtime can be identified in the data, due to the characteristic response of the APV25, by imposing thresholds on the common mode, $\text{CM} < -140$ ADC counts, and the cluster signal, $Q_{\text{CLU}} > 500$ ADC counts.

The *HIP rate*, the rate at which non-negligible deadtime is observed, is calculated by normalising the number of highly ionising events resulting in deadtime, N_{HIP} , to the factor $(N_{\text{TRIG}} \cdot \langle N_{\pi/\mu} \rangle \cdot N_{\text{PLANE}})$, where N_{TRIG} is the number of

triggered events, $\langle N_{\pi/\mu} \rangle$ is the mean pion (muon) multiplicity and N_{PLANE} is the number of detectors used to collect the data. Table 1 lists measurements of the HIP rate (per bunch crossing per particle per sensor plane) for pion and muon beams.

Table 1: HIP rate calculations

Beam	N_{TRIG}	$\langle N_{\pi/\mu} \rangle$	N_{PLANE}	N_{HIP}	R_{HIP}
Pion	244986	1.9	5	955	$(4.1 \pm 0.1) \cdot 10^{-4}$
Pion	215938	2.0	5	858	$(4.0 \pm 0.1) \cdot 10^{-4}$
Muon	225000	1.9	5	7	$(3.3 \pm 1.2) \cdot 10^{-6}$

As muons cannot interact hadronically, collisions between muons and silicon nuclei rarely generate the largest energy depositions, resulting in a negligible HIP rate measurement for incident muons.

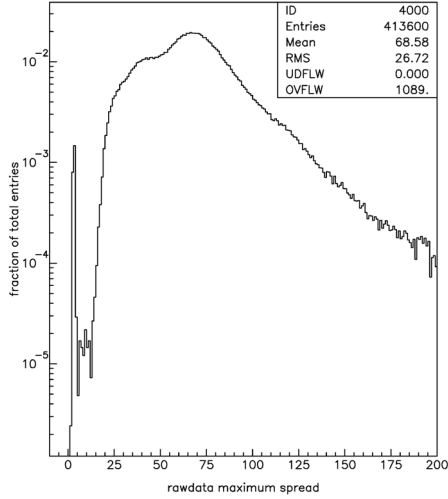


Figure 6: Absolute spread [ADC counts] in raw analogue data of an APV25 frame.

B. Deadtime measurement with pion beam

‘Disabled’ APV25 chips, which are experiencing deadtime after a highly ionising event, are also identifiable in the data, as the APV25 data frames contain baselines shifted to the lower limit of the APV25 dynamic range and no signal in any of the 128 channels or pedestal structure. This is clearly seen in figure 6, which shows the distribution of the peak-to-peak spread in the 128 analogue values of an APV25 frame. The peak observed at < 5 ADC counts is a consequence of fully suppressed baselines with no signal or pedestal structure. Normally, pedestal structure and the presence of signals result in a minimum peak-to-peak spread of ~ 15 ADC counts. Therefore, disabled APV25 chips are identified by imposing thresholds on the common mode, $\text{CM} < -140$ ADC counts, and the peak-to-peak spread in the raw data, $\delta < 10$ ADC counts.

Deadtime cannot be measured on an event-by-event basis (where ‘event’ here means a highly ionising event) with the X5 data, but an event-averaged value can be obtained by considering how the probability of observing a disabled APV25 in the analogue data from a triggered event depends on the trigger position within the SPS orbit.

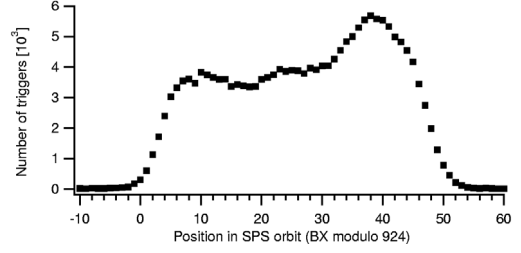


Figure 7: Distribution of trigger position in the SPS orbit.

Figure 7 shows the distribution of trigger positions in the SPS orbit with 120 GeV pions. The triggers are confined to the same ~ 60 RF buckets within the SPS orbit during a spill, which corresponds to the length of the particle bunch trains. Figures 8 (a) and (b) show the number of highly ionising events and disabled APV25 chips observed in the data as a function of trigger position. The difference in statistics for figures 8 (a) and (b) is due to the increased probability of observing a disabled APV25 due to the non-zero deadtime. Normalising these two distributions to the trigger distribution in figure 7 provides the probability of observing a highly ionising event / disabled APV25 as a function of trigger position, as shown in figures 9 (a) and (b), respectively.

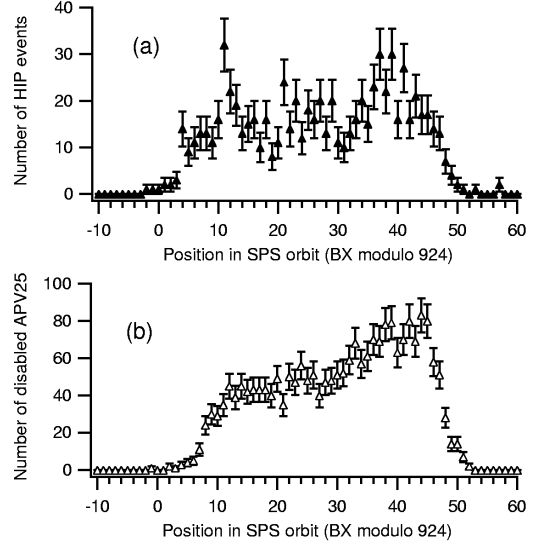


Figure 8: (a) Distribution of highly ionising events as a function of trigger position in the SPS orbit. (b) Distribution of disabled APV25s as a function of trigger position in the SPS orbit.

As seen in figure 9 (a), the probability of observing a highly ionising event is constant at $\sim 4 \cdot 10^{-3}$ during the bunch train and zero before and after. Normalising this probability to the number of sensor planes (5) and the pion multiplicity (1.9) provides a HIP rate measurement of $\sim 4 \cdot 10^{-4}$ per bunch crossing per pion per plane, which is in good agreement with earlier HIP rate measurements with pions, listed in table 1.

The probability of observing a disabled APV25 depends on the probability of a highly ionising event occurring in the preceding bunches of the train. Importantly, trains of $\sim 1.5\mu\text{s}$ length arrive at the target area every SPS orbit period ($23.1\mu\text{s}$) and so are sufficiently spaced such that highly ionising events occurring in one train cannot contribute to any

deadtime observed in the following train. Therefore, the probability of observing a disabled APV25 is zero at the beginning of a train (as there are no preceding triggers). This probability increases as the trigger position moves further into the train, due to the increasing probability of observing a highly ionising event, and then saturates. Saturation occurs because only highly ionising events that precede a trigger by a time interval less than the induced deadtime can contribute to the probability of a trigger containing a disabled APV25. The time taken for the probability to saturate provides a measure of the average deadtime.

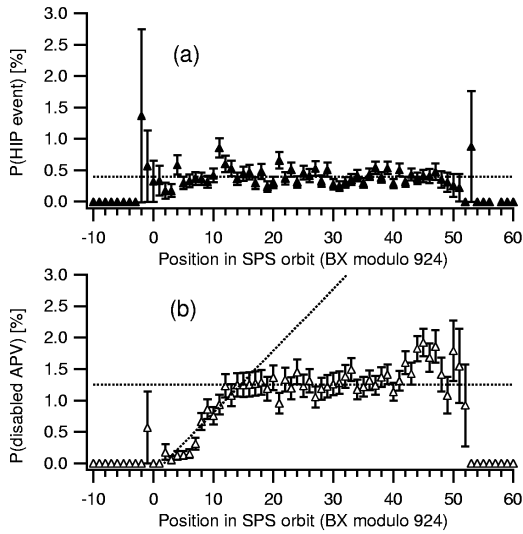


Figure 9: (a) Probability of a trigger containing a highly ionising event as a function of trigger position in the particle bunch trains. (b) Probability of a trigger containing a disabled APV25 as a function of trigger position in the particle bunch trains.

Figure 9 (b) shows the probability of observing a disabled APV25 as a function of trigger position. The deadtime, obtained from the time taken for the probability to saturate, is 13 ± 2 [25 ns intervals] or, equivalently, 325 ± 50 ns.

III. LABORATORY MEASUREMENTS

Highly ionising events were simulated in the laboratory by injecting large signals directly into a number of APV25 channels. Adjacent channels were coupled to these large signals through a capacitor network to simulate inter-strip capacitive coupling. After some delay, a 3-MIP signal was then injected into another channel and the APV25 triggered a latency period later to read out the amplitude of the 3-MIP signal. Measurements were repeated for different delays (up to 5 μ s, in 0.1 μ s steps) to obtain the amplitude of the 3-MIP signal as a function of time after the simulated highly ionising event. The resulting deadtime was defined to be the time interval for which zero signal amplitude was observed. Deadtime measurements were made for a range of simulated energy depositions (5 to 100 MeV), with the signal injected either on 1 channel or shared between 2 channels.

Figure 10 shows the measured deadtime as a function of the simulated energy deposition, when collected on one or two strip(s) and for two values of R_{INV} . The signal magnitude

is accurate to ± 5 % (this error is largely attributable to the non-negligible tolerance of the charge injection capacitors) and the deadtime measurement is accurate to ± 5 ns.

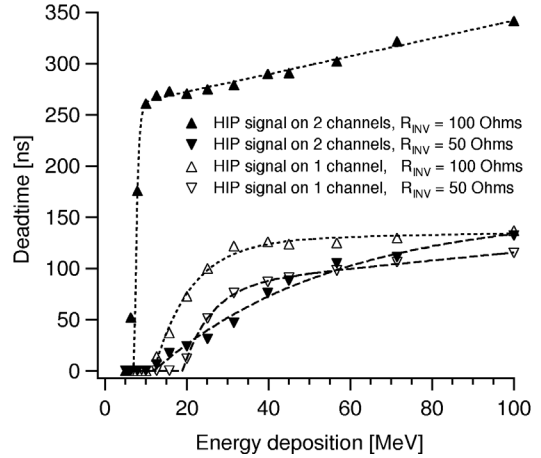


Figure 10: Deadtime [ns] as a function of signal magnitude [MeV], when injected on 1 and 2 strip(s) and for 2 values of R_{INV} .

These studies have shown that the measured deadtime for a given energy deposition is reduced by decreasing the value of the external resistor, R_{INV} . The maximum observed deadtime is reduced from ~ 350 ns to ~ 100 ns when R_{INV} is reduced from 100 Ω to 50 Ω . Further, the threshold energy deposition required for non-negligible deadtime is increased from 7 MeV to 12 MeV. Importantly, the observed deadtime with $R_{INV} = 100$ Ω is strongly dependent on how the signal is shared between channels; this dependence is reduced with $R_{INV} = 50$ Ω .

The cumulative energy deposition spectra, shown in figure 1 (b), can be used in conjunction with the laboratory-measured 7 MeV threshold to predict the probability of a π -Si interaction resulting in non-negligible deadtime; a value of $\sim 8 \cdot 10^{-4}$ is obtained for 120 GeV pions, which is in good agreement with the experimentally measured HIP rate at X5, as listed in table 1.

IV. PSI BEAM TEST

A further beam test at PSI in May 2001 was dedicated to studying the HIP effect in more detail. The readout system comprised of 12 readout silicon sensors, each instrumented with 4 APV25 chips, and electrical readout to 3 FED-PMC cards housed in 2 PCs. The sensors were exposed to a continuous 200 MeV pion beam with a 50 MHz bunch structure, similar to the environment expected in CMS (the most probable pion energy predicted for CMS is ~ 300 MeV [3]). Due to the 50 MHz bunch structure, particles were coincident in time with the 40 MHz readout cycle only every 100 ns, therefore triggers generated by scintillator coincidence were confined to this periodicity to ensure both the beam and readout clocks were in phase.

The aims of the beam test were three-fold: to perform HIP rate measurements in a CMS-like environment; to investigate in detail the full recovery of an APV25 after a highly ionising event; and to perform HIP rate and deadtime measurements with modules using a reduced hybrid resistor (R_{INV}) value.

In order to investigate the APV25 recovery, a custom-built trigger card was designed to provide bursts of triggers spaced by 75 ns to the readout electronics. In conjunction with this trigger configuration, the APV25 chips were operated in multi-mode, providing readout from three consecutive 25 ns intervals per trigger, and thus providing data every 25 ns for 750 ns.

Table 2: Preliminary HIP rate measurements for various module types (Tracker Inner / Outer Barrels and Endcap) and R_{INV} values.

Module type	Sensor thickness [μm]	R_{INV} [Ω]	R_{HIP} (10^{-4})
TIB	320	50	2.3 ± 0.1
TIB	320	100	3.7 ± 0.1
TOB	500	50	5.5 ± 0.1
TOB	500	75	5.8 ± 0.2
TOB	500	100	6.2 ± 0.1
TEC	500	100	6.2 ± 0.1

Table 2 lists preliminary measurements of the HIP rate [per bunch crossing per pion per plane] for different module types and values of R_{INV} . The factor ~ 0.6 between the HIP rates for the TIB and TOB/TEC modules reflects the different thicknesses of the sensors. The HIP rate is also seen to decrease slightly as R_{INV} is reduced.

Measurements have been made regarding the recovery of the APV25 after a highly ionising event and preliminary results suggest that the inefficiencies introduced by highly ionising events are at the sub-% level.

V. INEFFICIENCIES DUE TO HIGHLY IONISING EVENTS

As discussed earlier, deadtime in the APV25 caused by highly ionising events can result in the loss of signal from minimum ionising particles. For a given energy deposition E_{DEP} [MeV] in a silicon sensor, the resulting inefficiency, $\epsilon(E_{DEP})$ [per % occupancy per sensor plane] is given by:

$$\epsilon(E_{DEP}) = 128 \times \eta \times P(E_{DEP}) \times \frac{\Gamma(E_{DEP})}{25 \text{ ns}} \quad (\text{equ. 1})$$

where $P(E_{DEP})$ is the probability of an energy deposition E_{DEP} , $\Gamma(E_{DEP})$ [ns] is the deadtime resulting from the energy deposition E_{DEP} , η [%] is the particle occupancy and the factor 128 accounts for all 128 channels of an APV25 being disabled. The total inefficiency, ϵ_{TOT} , is obtained by summing $\epsilon(E_{DEP})$ over all energy depositions, E_{DEP} .

A prediction of the inefficiencies for the CMS environment can be made using the results presented above. The spectra shown in figure 1 (a) provide the probability, $P(E_{DEP})$, of a π -Si interaction resulting in an energy deposition E_{DEP} . Fits to the laboratory measurements of deadtime versus

energy deposition (figure 10) provide the deadtime, $\Gamma(E_{DEP})$, resulting from an energy deposition E_{DEP} . Table 3 summarises the total inefficiencies expected at both X5 and in the CMS Tracker Inner and Outer Barrel regions.

Table 3: Inefficiency, ϵ_{TOT} , [per % occupancy per plane] for various environments and R_{INV} values.

R_{INV} [Ω]	ϵ_{TOT} [per % occupancy per sensor plane]		
	X5	TIB	TOB
100	0.0104	0.0072	0.0052
50	-	0.0050	0.0003

VI. CONCLUSIONS

Highly ionising events in silicon sensors can cause measurable deadtime in the APV25 readout chip. For extremely large signals, $\gg 100$ minimum ionising particles, all 128 channels of the APV25 chip are affected, due to the design of the biasing at the APV25 inverter stage.

The effect of highly ionising events on the APV25 has been studied with analysis of data from two beam tests, in the laboratory and with simulation. All results obtained from these studies are in good agreement. The rate at which non-negligible deadtime is observed is $< 10^{-3}$ and the deadtime resulting from highly ionising events is of the order ~ 300 ns.

The inefficiency due to highly ionising events has been predicted for the CMS environment, using results from simulation and laboratory measurements, and is at the sub-percent level. Preliminary results from the PSI beam test suggest inefficiencies at the sub-percent level with CMS-like operating conditions.

Laboratory measurements predict that deadtime for a given energy deposition may be reduced by decreasing the value of an external hybrid resistor, but this has yet to be confirmed by analysis of beam test data.

VII. ACKNOWLEDGEMENTS

The author would like to thank all involved in the X5 and PSI beam tests for their important contributions to this study, and to M. Raymond for his work on the APV25 deadtime measurements.

The author would also like to thank the UK Particle Physics and Astronomy Research Council for their financial support of his work.

VIII. REFERENCES

- [1] M. Huhtinen, *Highly ionising events in silicon detectors*, CMS Note 2002/011
- [2] M. Bozzo et al., *Observation of the slow-extracted 25 ns bunched beam*, Proceedings of Chamonix XI, January 2001
- [3] *The Tracker Project TDR*, CERN/LHCC 98-6